Inhibition of SGLT2 Rescues Bone Marrow Cell Traffic for Vascular Repair: Role of Glucose Control and Ketogenesis

Mattia Albiero,[1,2] Serena Tedesco,[1,2] Francesco Ivan Amendolagine,[2] Marianna D'Anna,[1,2] Ludovica Migliozzi,[1,2] Gaia Zuccolotto,[3,4] Antonio Rosato,[3,4] Roberta Cappellari,[1,2] Angelo Avogaro,[1] and Gian Paolo Fadini[1,2]

Diabetes 2021;70:1767–1779 | https://doi.org/10.2337/db20-1045

The mechanisms by which sodium–glucose cotransporter 2 inhibitors (SGLT2i) improve cardiovascular outcomes in people with diabetes are incompletely understood. Recent studies show that SGLT2i may increase the levels of circulating cells with vascular regenerative capacity, at least in part by lowering glycemia. In this study, we used mice with streptozotocin-induced diabetes treated with the SGLT2i dapagliflozin at a dose that reduced glucose levels by 20%. Dapagliflozin improved the diabetes-associated defect of hematopoietic stem cell mobilization after stimulation with granulocyte colony-stimulating factor. Dapagliflozin rescued the traffic of bone marrow (BM)–derived cells to injured carotid arteries and improved endothelial healing in diabetic mice. Defective homing of CD49d$^+$ granulocytes was causally linked with impaired endothelial repair and was reversed by dapagliflozin. The effects of dapagliflozin were mimicked by a similar extent of glucose reduction achieved with insulin therapy and by a ketone drink that artificially elevated β-hydroxybutyrate. Inhibition of endothelial repair by resident cells using the CXCR4 antagonist AMD3100 did not abolish the vascular effect of dapagliflozin, indirectly supporting that endothelial healing by dapagliflozin was mediated by recruitment of circulating cells. In summary, we show that dapagliflozin improved the traffic of BM-derived hematopoietic cells to the site of vascular injury, providing a hitherto unappreciated mechanism of vascular protection.

The primary consequence of diabetes is the accelerated development of cardiovascular disease (1), driving a huge burden for affected individuals, health care systems, and society. Unlike microangiopathies (i.e., retinopathy, nephropathy, and neuropathy), cardiovascular complications can marginally be prevented by achieving near-normal glucose levels (2).

The demonstration that treatment with sodium–glucose contransporter 2 inhibitors (SGLT2i) improves cardiovascular outcomes of diabetes (3) represented the major groundbreaking finding in the last 10 years of research in the field. Despite huge efforts, the mechanisms by which SGLT2i protect from the adverse cardiovascular consequences of hyperglycemia have not been elucidated (4). The simultaneous effect of SGLT2i on multiple risk factors (glycemia, blood pressure, and obesity) only accounts for part of the observed cardiovascular benefit (5). Since SGLT2i exert much of their protection against heart failure, the atypical natriuretic action has been hypothesized to be primarily involved (6). Yet, this would not explain the delayed mortality observed in patients with diabetes and cardiovascular disease who received SGLT2i (7). Interestingly, SGLT2i is associated with an increase in hematocrit (8), which appeared to be mediating the delay in cardiovascular death (9,10). Inhibition of the cardiac

[1]Department of Medicine, University of Padova, Padova, Italy
[2]Veneto Institute of Molecular Medicine, Padova, Italy
[3]Department of Surgery, Oncology and Gastroenterology, University of Padova, Padova, Italy
[4]Istituto Oncologico Veneto–Istituto di Ricovero e Cura a Carattere Scientifico, Padova, Italy

Corresponding author: Gian Paolo Fadini, gianpaolo.fadini@unipd.it

Received 14 October 2020 and accepted 21 April 2021

This article contains supplementary material online at https://doi.org/10.2337/figshare.14465508.

M.A. and S.T. equally contributed to this work.

See accompanying article, p. 1620.

sodium/potassium exchanger by SGLT2i has been shown in vitro (11) and might protect the heart from ischemic injury, but its clinical relevance remains unclear. Another candidate mediator of cardioprotection by SGLT2i is the switch to ketone body utilization (12), which would improve myocardial energetics (13).

Lastly, it has been hypothesized that SGLT2i may stimulate circulating hematopoietic stem/progenitor cells (HSPCs). Low levels of circulating HSPCs with vascular tropism have been consistently reported in both type 1 diabetes (T1D) and type 2 diabetes (T2D) (14), which is considered to contribute to cardiovascular damage (15). Prior studies indicate that low HSPC levels are due to an impaired mobilization from the bone marrow (BM) to peripheral blood (16). Such stem cell "mobilopathy" (17) is driven by a combination of BM remodeling (microangiopathy and neuropathy) and inflammation (14,18), with functional pathways that can be targeted by specific therapies (19). In patients with T2D, Hess et al. (20) reported that the SGLT2i empagliflozin increased expression of the HSPC marker CD133 on aldehyde dehydrogenase–expressing cells, which are supposed to be provided with vasculotropic properties. On the contrary, we found that effect of SGLT2i on antigenically defined HSPCs and endothelial precursors are mostly related to the improved glucose control (21,22).

In this study, we used mouse models to evaluate if the SGLT2i dapagliflozin can improve traffic of HSPCs from the BM to sites of vascular damage in diabetes. We also explored some systemic pathways that could explain the effects of dapagliflozin on HSPCs and their vascular effect.

RESEARCH DESIGN AND METHODS

Mice

C57BL/6J wild-type (Wt) and C57BL/6-Tg(UBC-GFP) mice were purchased from The Jackson Laboratory and established as a colony since 2001 and 2017, respectively. Mice were randomly assigned to treatments or experimental groups. All animal studies were approved by the Animal Care and Use Committee of the Veneto Institute of Molecular Medicine and by the Italian Health Ministry.

Induction of Diabetes

Three- to 4-month-old male mice were used. Type 1-like diabetes was induced by a single i.p. injection of 175 mg/kg streptozotocin (STZ) in 100 mmol/L, pH 4, Na-citrate buffer (23). Blood glucose, ketones (β-hydroxybutyrate [BOHB]), and urinary glucose were measured using a point-of-care device (FreeStyle; Abbott, Abbott Park, IL). Diabetes onset was confirmed for blood glucose ≥300 mg/dL 48 h after STZ injection, but only mice with persistent hyperglycemia in the subsequent 2 weeks were used.

Type 2-like diabetes was induced by feeding mice with a high-fat diet (HFD) (60% of the total energy derived from fat) (ssniff EF, acc. D12492 [I] mod.; Spezialdiäten, Soest, Germany) for 6 weeks. To verify dysmetabolism, an i.p. glucose tolerance test was performed by injecting 1 g/kg glucose i.p. and measuring blood glucose at 0, 30, 60, and 120 min.

Two weeks after the onset of diabetes (STZ) or 4 weeks after initiation of HFD, dapagliflozin (AstraZeneca) was administered in the drinking water at a dosage of 5 mg/kg/day for 2 weeks.

Carotid Endothelial Damage

Mice were anesthetized with inhaled isoflurane. The left common carotid artery was exposed and injured by applying an electric current with a bipolar tweezer for 4 mm from the branching. Three days later, the extent of residual endothelial damage was evaluated by tail vein injection of 200 μL of 5% Evans blue. Mice were then killed by overdose of inhaled carbon dioxide, perfused with PBS to remove blood and excess staining, and both carotid arteries were excised, placed between glass slides with mounting medium, and photographed with a light microscope. In BM transplantation experiments, at sacrifice, carotid arteries were excised and processed with 0.025% trypsin-EDTA (Merck), 2 mg/mL collagenase II (Worthington Biochemical Corporation), and 60 units/mL of DNase (Merck) for 1 h at 37°C to obtain a cell suspension for flow cytometry.

BM Transplantation

Recipient mice were treated with a myeloablative total-body irradiation with 10 Gy, split in two doses of 5 Gy 3 h apart, and followed by intravenous injection of BM cells from donor C57BL/6-Tg(UBC-GFP) mice (10^7/each) isolated by flushing femurs and tibias with sterile ice-cold PBS. Animals were housed with sterile cages, water, food, and bedding for 4 weeks to allow BM reconstitution. Engraftment was assessed by peripheral blood cell count. Complete engraftment and development of the BM-GFP chimera were confirmed when ≥95% of white blood cells (WBC) were GFP^+.

Treatments

Treatment with the SGLT2i dapagliflozin was initiated 2 weeks after confirming the onset of STZ diabetes. Dapagliflozin (AstraZeneca) was given in the drinking water at a dosage of 5 mg/kg/day for 2 weeks. HSPC mobilization was induced by injecting animals subcutaneously with 200 mg/kg/day human recombinant granulocyte colony-stimulating factor (G-CSF) daily for 4 consecutive days. CD49d blockade was performed by injecting the animals daily intravenously with 30 μg of an anti-mouse CD49d antibody (clone R1–2; Thermo Fisher Scientific) from day −1 through day 3 after carotid injury. AMD3100 (Tocris Bioscience) was given by daily subcutaneous injections of 1.25 mg/kg for 3 days. In a set of experiments, diabetic mice were treated with 1.5 units/day of insulin glargine (Eli Lilly and Company) for 2 weeks by daily i.p. injection. Ketone supplement (Keto BHB Salts Supplement; Zenwise

Health, Wilmington, DE) was added to the drinking water at 5 g/kg/day for 2 weeks.

Hematologic Characterization

Total WBC count was performed using the CELL-DYN Emerald Hematology Analyzer (Abbott) on fresh EDTA-treated mouse blood. For measuring circulating erythropoietin (EPO), EDTA-treated blood samples were centrifuged at 2,000*g* for 10 min to obtain plasma that was stored at −20°C. Plasma EPO was quantified using the Mouse Erythropoietin Quantikine ELISA Kit (R&D Systems, Minneapolis, MN) according to the manufacturer's instructions.

For colony-forming unit (CFU) assay, BM cells (3×10^4) were plated in 35-mm Petri dishes containing 1 mL methylcellulose-based medium MethoCult supplemented with 1% penicillin/streptomycin. Alternatively, after red blood cell (RBC) lysis, 25 μL of peripheral blood were plated in 24-well plates containing 0.5 mL MethoCult (Voden) supplemented with 1% penicillin/streptomycin. Colony formation was scored after 10 days of culture. In separate experiments, dapagliflozin at different concentrations was added to the MethoCult medium.

Flow cytometry was performed on murine BM cells, EDTA-treated peripheral blood, or cell suspensions, as needed. BM cells were isolated from femurs and tibiae by flushing the bone cavity with ice-cold PBS through a 40 μmol/L cell strainer. A total of 100 μL of BM cell suspension, peripheral blood cells, or cells from carotid arteries was labeled with specific antibodies, as reported in Supplementary Table 1.

Histology

The 10-mm–thick kidney and femur cryosections were obtained with a Leica CM1950 cryostat (Leica Biosystems, Milan, Italy). Sections were incubated with anti-rabbit anti–SGLT2 polyclonal antibody and after with goat anti-rabbit Cy3 (catalog number 111-165-003; Jackson ImmunoResearch Laboratories, West Grove, PA). Nuclei were counterstained with Hoechst 33352. Images were taken with a Leica DM6 B microscope and then processed with Fiji/ImageJ 1.50 software (National Institutes of Health, Bethesda, MD).

Western Blot

Human umbilical vein endothelial cells (HUVECs) were seeded in six-well plates with complete Endothelial Cell Basal Medium (catalog number C-22210; PromoCell) supplemented with 10% FBS and 1% penicillin/streptomycin and glutamine (Corning). Upon reaching 80% confluence, cells were synchronized by serum starvation for 24 h. After that, cells were incubated with 0.5 μmol/L AMD3100 (catalog number 155148-31-5; Tocris Bioscience) for 2.5 h before stimulation for 30 min with 20 ng/mL human CXCL12 (catalog number 350-NS; R&D Systems). Cells were lysed on ice with modified radioimmunoprecipitation assay lysis buffer (50 mmol/L Tris-HCl, 150 mmol/L NaCl, 10 mmol/L $MgCl_2$, 0.5 mmol/L DTT, 1 mmol/L EDTA, and 10% glycerol) supplemented with 1% Triton X-100, 1% SDS, cOmplete Protease Inhibitor Cocktail (Roche), and Phosphatase Inhibitor Cocktails 2 and 3 (Merck). Lysates were heated at 70°C for 10 min, and, after centrifugation at 13,000*g* for 15 min, protein was quantified in supernatants using the BCA assay (Thermo Fisher Scientific). Proteins (10 μg) were separated on 10% SDS-PAGE and transferred onto nitrocellulose membranes. Membranes were then blocked and probed using the following primary antibodies: rabbit anti–phospho-AktSer473 antibody (1:1,000; #9271; Cell Signaling Technology, Danvers, MA), rabbit anti-Akt (1:1,000; #9272; Cell Signaling Technology), and mouse anti-GAPDH (1:10,000; ab8245; Abcam, Cambridge, U.K.). After washing, membranes were incubated with appropriate secondary horseradish peroxidase–conjugated antibodies (all from Jackson ImmunoResearch Laboratories). Bands were detected by chemiluminescence using the WesternBright Quantum HRP substrate (Advansta, Inc., Menlo Park, CA). Images were acquired with an ImageQuant LAS 4000 (GE Healthcare, Chicago, IL). Densitometric analysis was performed with ImageJ 1.47v (National Institutes of Health).

Adhesion Assay

Fibroblasts were isolated from skin explants of Wt mice and cultivated with DMEM 5 mmol/L glucose medium (Merck) supplemented with 10% FBS (Corning) and 1% L-glutamine/penicillin-streptomycin (Corning). Cells were seeded in 12-well plates until 100% confluent. Total BM was isolated from C57BL/6-Tg(UBC-GFP) mice by flushing femurs and tibias with sterile ice-cold PBS. GFP^+ Ly6G/Cmid/low Siglec-F^+ cells were sorted and incubated with 2 μg of anti-mouse CD49d antibody (clone R1–2) or isotype IgG2bk antibody for 45 min at 37°C. Cells were then plated on fibroblasts for 2 h. Nonadherent cells were removed by a gentle wash with PBS followed by fixation with 4% paraformaldehyde before imaging.

Gene Expression

RNA was isolated from flushed BM or cells by use of QIAzol or with a Total RNA Purification Micro Kit (Norgen Biotek Corp.) and quantified with a NanoDrop 2000 Spectrophotometer (Thermo Fisher Scientific). cDNA was synthesized from 500 ng RNA using a SensiFAST cDNA Synthesis Kit (Bioline, London, U.K.). Quantitative PCR was performed using SensiFAST SYBR Lo-ROX Kit (Bioline) via a QuantStudio 5 Real-Time PCR System (Thermo Fisher Scientific). The list of primers is given in Supplementary Table 2.

Statistical Analysis

Continuous data are expressed as mean ± SE unless otherwise specified. Normality was checked using the

Kolmogorov-Smirnov test, and nonnormal data were log-transformed before analysis. Comparison between two or more groups was performed using the Student *t* test and ANOVA for normal variables or the Mann-Whitney *U* test and Kruskal-Wallis test for nonnormal variables that could not be log-transformed (e.g., because of frequent zero values). To analyze data from experiments with two groups and two treatments, two-way ANOVA was used, and the effect of group and treatment was analyzed. All tests were two-tailed. Bonferroni adjustment was used to account for multiple testing. Biological replicates (individual mice) are shown as individual data points superimposed on bar charts. Significance was conventionally accepted at $P < 0.05$.

Data and Resource Availability

Data and resources used for this study are available from the corresponding author upon reasonable request.

RESULTS

Hematologic Effects of Dapagliflozin

We first evaluated gene expression of SGLT2 (*Slc5A2*) in various mouse organs and tissues relative to the ubiquitin housekeeping gene. BM cells constituted the extrarenal tissue with the highest gene expression of *Slc5A2*, followed by skeletal muscle and the heart (Supplementary Fig. 1*A*). *Slc5A2* expression was about three times higher in BM than in skeletal muscle, although it was four orders of magnitude lower ($10^{-}4$) than in the kidney (Supplementary Fig. 1*B*). We examined *Slc5A2* expression in hematopoietic versus mesenchymal precursor cells in vitro. Neither cultured hematopoietic CFUs nor isolated mesenchymal stem cells exhibited the same *Slc5A2* expression as BM cells freshly eluted from the bones (Supplementary Fig. 1*C*), suggesting that mature cells in the BM contributed most to *Slc5A2* expression. In fact, both mononuclear cells and polymorphonuclear cells had levels of *Slc5A2* expression similar to those of BM cells (Supplementary Fig. 1*C*). In view of the low *Slc5A2* gene expression, we were unable to detect SGLT2 protein expression in the BM by either flow cytometry (data not shown) or section immune staining (Supplementary Fig. 1*D*).

We then assessed the effects of inhibiting SGLT2 with dapagliflozin in STZ-induced diabetic mice (Fig. 1*A*). At the dose used, dapagliflozin increased urinary glucose more than fivefold in nondiabetic mice, confirming the pharmacologic effect (Fig. 1*B*). In STZ diabetic mice, urinary glucose was markedly elevated in untreated conditions and, at the end of the treatment period, was not further increased by dapagliflozin. Consistently, body weight was significantly lower in diabetic versus nondiabetic mice and was not affected by dapagliflozin (Fig. 1*C*). While dapagliflozin did not significantly reduce blood glucose levels in nondiabetic mice, it decreased blood glucose in diabetic mice on average from 437 to 349 mg/dL (equal to −20%; $P = 0.008$) (Fig. 1*D*). These results indicate that the extent of SGLT2 inhibition achieved was sufficient to elicit a pharmacologic response, but not to normalize glycemia in this model.

As expected, diabetes increased RBC count and hematocrit, an effect of hemoconcentration (Fig. 1*E* and *F*). As noted before, diabetes significantly increased the granulocyte/lymphocyte (G/L) ratio (Fig. 1*I*), a reflection of enhanced myelopoiesis induced by hyperglycemia (18,24). Dapagliflozin had no effect on RBCs, hematocrit, and platelets, while it increased WBC count in both diabetic and nondiabetic mice, but did not modify the G/L ratio (Fig. 1*E–I*). Within the BM, dapagliflozin modestly increased mature leukocytes (especially in nondiabetic mice) (Fig. 2*A*), while not affecting the generation of hematopoietic CFU in vivo (Fig. 2*B* and Supplementary Fig. 2*A*) or in vitro (Fig. 2*C* and Supplementary Fig. 2*B*). No change was also observed in primitive HSPCs expressing signaling lymphocyte activation molecule CD150 (SLAM) and various myeloid progenitors (Fig. 2*D* and *E*).

Dapagliflozin Partially Rescues HSPC Mobilization in Diabetic Mice

We previously reported that BM macrophages, especially those expressing the sialoadhesin CD169, retain HSPCs in the diabetic BM niche and prevent them from being mobilized in response to G-CSF (25). While not affecting the total number of macrophages (Fig. 3*A* and *B*), STZ diabetes increased $CD169^{+}$ BM macrophages up to 70%, an effect that was mostly abolished by dapagliflozin (Fig. 3*C* and *D*).

When stimulated with G-CSF, antigenically defined HSPCs (lineage $[Lin]^{-}c\text{-}kit^{+}Sca\text{-}1^{+}$ [LKS] cells) increased in nondiabetic mice by 7.3 ± 1.7-fold (Fig. 3*E*), paralleled by a marked increase in the generation of functionally defined HSPCs (CFU in Fig. 3*F*). As demonstrated before, diabetic mice were completely unresponsive to the HSPC-mobilizing effect of G-CSF, with no change in HSPCs (1.4 ± 0.5-fold) (Fig. 3*G*) and CFUs (Fig. 3*H*). Dapagliflozin did not significantly modify response to G-CSF in nondiabetic mice (Fig. 3*E* and *F*), while it partially rescued HSPC mobilization in STZ diabetic mice: in dapagliflozin-treated STZ diabetic mice, HSPC increased by 3.2-fold and generation of CFU increased by 4.5-fold (Fig. 3*G* and *H*). Thus, despite a modest effect on blood glucose, dapagliflozin prevented one pathologic feature of inflammatory BM alterations in STZ diabetes, namely the surge in $CD169^{+}$ macrophages, and partially rescued HSPC mobilization.

Dapagliflozin Improves Endothelial Healing in Diabetic Mice

Next, we examined if the partial rescue of HSPC mobilization translated into an improved traffic of BM-derived cells to sites of vascular damage using the carotid damage model. Endothelial injury was induced experimentally by a standardized low-voltage electrical current yielding a 4-

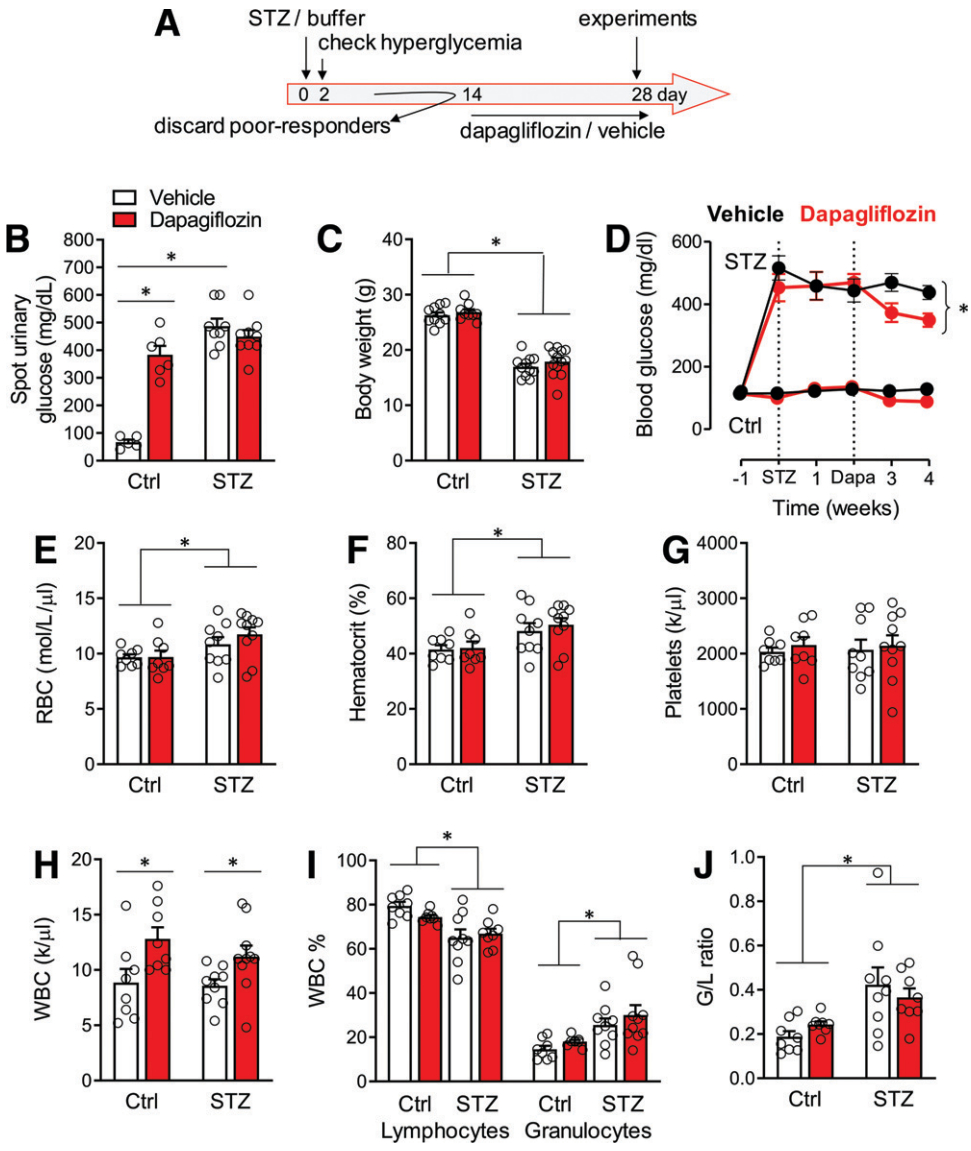

Figure 1—Hematologic effect of dapagliflozin. We examined the effects of 2-week dapagliflozin or vehicle administration in nondiabetic control (Ctrl) mice and STZ-induced diabetic mice (flowchart in *A*) on urinary glucose excretion (*B*), body weight (*C*), blood glucose levels (*D*), RBCs (*E*), hematocrit (*F*), platelets (*G*), absolute (*H*) and relative (*J*) WBC counts, and the G/L ratio (*I*). Histograms show mean and SE with superimposed data points for individual mice. Two-way ANOVA was first used, followed by post hoc *t* test (*$P < 0.05$ for the indicated comparison). Dapa, dapagliflozin.

mm denudation, which was stained with Evans blue. Re-endothelization in healthy mice normally reaches 50% at 3 days after injury and is evidenced by reduced Evans blue staining. As shown in Fig. 4*A*, spontaneous endothelial healing at day 3 after injury was dramatically reduced in STZ diabetic versus nondiabetic mice (5.5 ± 1.1% vs. 40.0 ± 1.3%; $P < 0.001$), while it was improved in diabetic mice treated with dapagliflozin (16.9 ± 4.0%; $P = 0.02$ vs. diabetic mice receiving vehicle). Yet, the extent of endothelial healing in diabetic mice treated with dapagliflozin was still significantly lower than in nondiabetic mice ($P < 0.01$).

In type 2-like diabetic mice induced by HFD, despite fasting and postload hyperglycemia (Supplementary Fig. 3*A* and *B*), HSPC mobilization was preserved and enhanced compared with control mice (Supplementary Fig. 3*D* and *E*), and there was no defect in re-endothelization (Supplementary Fig. 3*F*). Dapagliflozin normalized glucose levels in HFD, induced ketogenesis, and dampened HSPC mobilization (Supplementary Fig. 3*A*–*E*). However, the lack of mobilopathy, which has been shown before in models of type 2 diabetes (18,26), along with unaffected endothelial healing (Supplementary Fig. 3*F*), makes the HFD model unsuitable to evaluate the role of dapagliflozin on HSPC traffic and vascular repair.

Having shown that dapagliflozin improved vascular healing in STZ diabetes, we then evaluated the traffic of

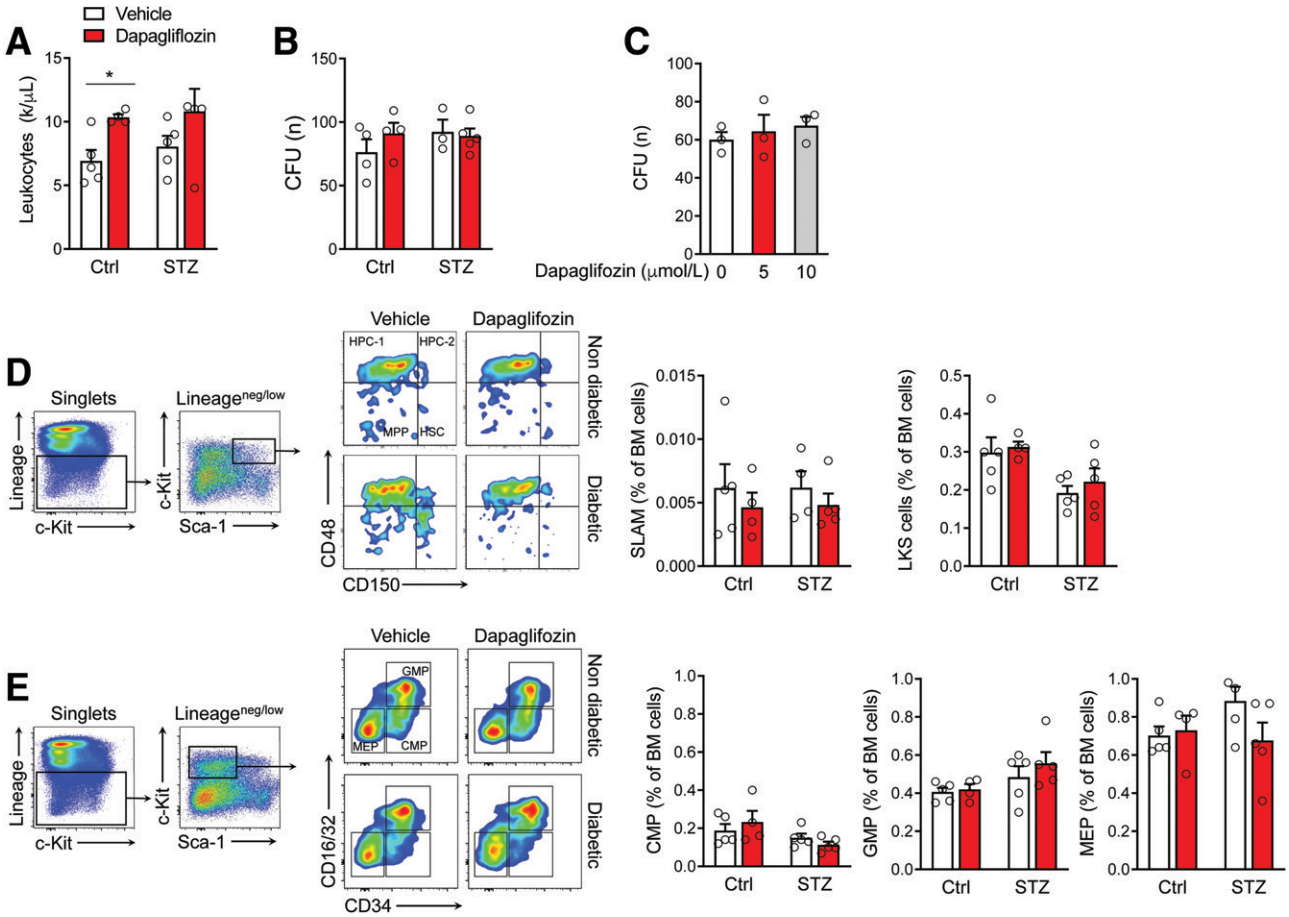

Figure 2—Effects of dapagliflozin inhibition on BM cells. Effects of dapagliflozin or vehicle administration in nondiabetic control (Ctrl) mice and STZ-induced mice induced on BM leukocytes (*A*) and CFUs and from BM cells (*B*). *C*: Treatment of BM cells with dapagliflozin at 0 (vehicle), 5, and 10 μmol/L during the CFU assay. *D*: Effects of dapagliflozin on HSPCs, defined as LKS, and BM primitive hematopoietic stem cells (SLAM) defined as LKS and by the additional markers CD48 and CD150. The right panel in *D* shows quantification in the various groups. *E*: Effects of dapagliflozin on BM common myeloid progenitors (CMP), granulocyte-monocyte progenitors (GMP), and megakaryocyte-erythroid progenitors (MEP) defined by flow cytometry based on the expression of Sca-1, c-kit, and Lin markers, CD34 and CD16/CD32. The right panel in *E* shows quantification in the various groups. Histograms show mean and SE with superimposed data points for individual mice. Two-way ANOVA was first used, followed by post hoc *t* test (*$P < 0.05$ for the indicated comparison).

BM-derived cells. To this end, we generated BM-GFP$^+$ chimeric mice by transplanting BM cells from mice ubiquitously expressing GFP into myeloablated Wt mice. After reconstitution, chimerism was always >95%, and there was no overt hematologic disturbance (Supplementary Fig. 4). Chimeric mice were rendered diabetic or kept nondiabetic by injecting them with STZ or vehicle, respectively. After 4 weeks, we performed carotid endothelial damage under treatment with dapagliflozin or vehicle. At day 3 after injury, we evaluated the accumulation and phenotype of BM-derived GFP$^+$ cells homed to the damaged carotids (Fig. 4*B*). Upon immunofluorescence staining of whole mount carotids, there was clear evidence of abundant GFP$^+$ cells (Fig. 4*B*). Using flow cytometry, we found that, in nondiabetic mice, GFP$^+$ cells were more than doubled at day 3 postinjury compared with the uninjured carotid, whereas this effect was completely absent in vehicle-treated diabetic mice. Dapagliflozin treatment rescued homing of GFP$^+$ cells to the injured carotids toward normal levels (Fig. 4*C*). Injury increased HSPCs in the carotid wall of nondiabetic mice, whereas it did not in diabetic mice, even under dapagliflozin treatment (Fig. 4*D*). However, antigenically defined HSPCs (LKS cells) accounted for 0.1% of GFP$^+$ cells homed to the damage site, whereas most GFP$^+$ cells were mature cells, especially granulocytes and monocytes, with a minority assuming the macrophage phenotype (Fig. 4*E*). GFP$^+$ macrophages were increased at sites of endothelial injury by treating diabetic mice with dapagliflozin (Fig. 4*E*), although they still represented a minority of total GFP$^+$ cells. Among mature cells, we then focused on CD49d$^+$ granulocytes, which we have recently found to be a provascular cell phenotype impaired in human and murine diabetes and rescued by dapagliflozin (27). After carotid endothelial injury, CD49d$^+$ granulocytes (mostly Gr-1$^+$) represented 4–5% of homed cells in nondiabetic mice, were significantly reduced in STZ diabetic mice to <2% ($P < 0.001$), and were rescued by dapagliflozin (Fig. 4*F*). To explore

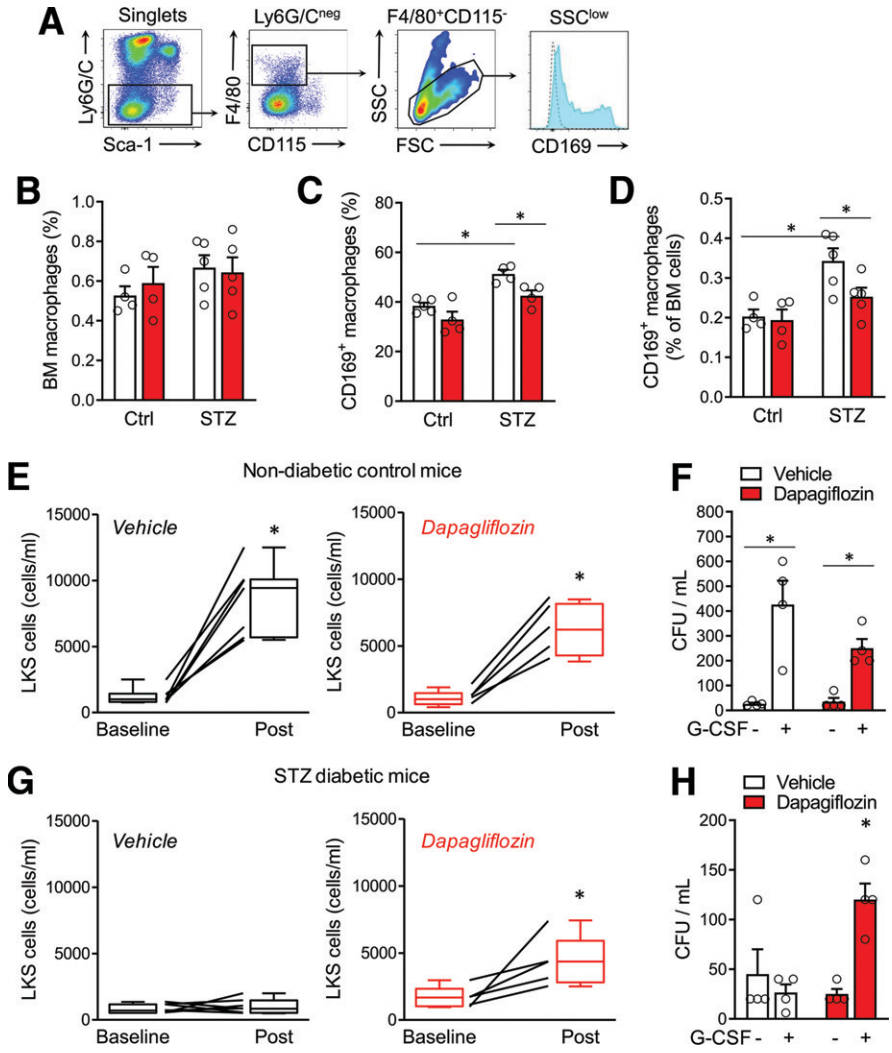

Figure 3—Effects of dapagliflozin inhibition on HSPC mobilization. *A* shows the flow cytometry gating strategy used to enumerate BM macrophages and their CD169$^+$ fraction. *B* through *D* show the percentage of macrophages over total BM cells (*B*), the percentage expression of CD169 on BM macrophages (*C*), and the percentage of CD169$^+$ macrophages over total BM cells (*D*). Mobilization of antigenically defined HSPCs (LKS cells) in nondiabetic (*E*) and diabetic (*G*) mice under vehicle or dapagliflozin treatment. Levels of functionally defined HSPCs (CFUs) obtained from peripheral blood cells in nondiabetic (*F*) and diabetic (*H*) mice under vehicle or dapagliflozin treatment (*$P < 0.05$ vs. vehicle upon paired test). In *B–D*, *F*, and *H*, histograms show mean values, SEs, and superimposed individual data points. Two-way ANOVA was first used, followed by post hoc *t* test (*$P < 0.05$ for the indicated comparison). In *E* and *G*, box plots show median (line), interquartile range (box), and range (whiskers) with connecting lines representing individual mice (*$P < 0.05$ post vs. baseline upon paired test). Ctrl, control; FSC, forward light scatter; SSC, side scatter.

mechanistic salience of this finding, we performed additional experiments on CD49d$^+$ cells. G-CSF induced a significant mobilization of CD49d$^+$ neutrophils but not eosinophils, without any modification by STZ diabetes (Fig. 5*A*). We then examined if defective homing of CD49d$^+$ cells was causally linked to impaired re-endothelization. We isolated Ly6G^{low}Siglec-F$^+$ granulocytes from GFP-transgenic mice, as a population enriched in CD49d$^+$ cells, and examined their adhesion capacity (Fig. 5*B*). Blocking CD49d with a neutralizing monoclonal antibody (mAb) impaired adhesion of these cells to fibroblasts in vitro (Fig. 5*C*). Then, we blocked CD49d in vivo by injecting the mAb in nondiabetic mice undergoing carotid endothelial injury. Compared with vehicle-treated mice, those receiving anti-CD49d mAb displayed a significantly lower re-endothelization (Fig. 5*D*), suggesting that homing of CD49d$^+$ cells is required for normal endothelial healing.

Endothelial healing occurs through two different mechanisms: *1*) migration of resident endothelial cells; and *2*) recruitment of circulating BM-derived cells. As CXCR4 is involved in these processes (28,29), we investigated whether CXCR4 was implicated in the effects of dapagliflozin on BM cell homing and endothelial repair. To this end, we blocked CXCR4 signaling with AMD3100 at a dose (1.25 mg/kg for 3 days) that did not stimulate HSPC mobilization and release of CD49d$^+$ neutrophils (Supplementary Fig. 3). We first verified that in vitro

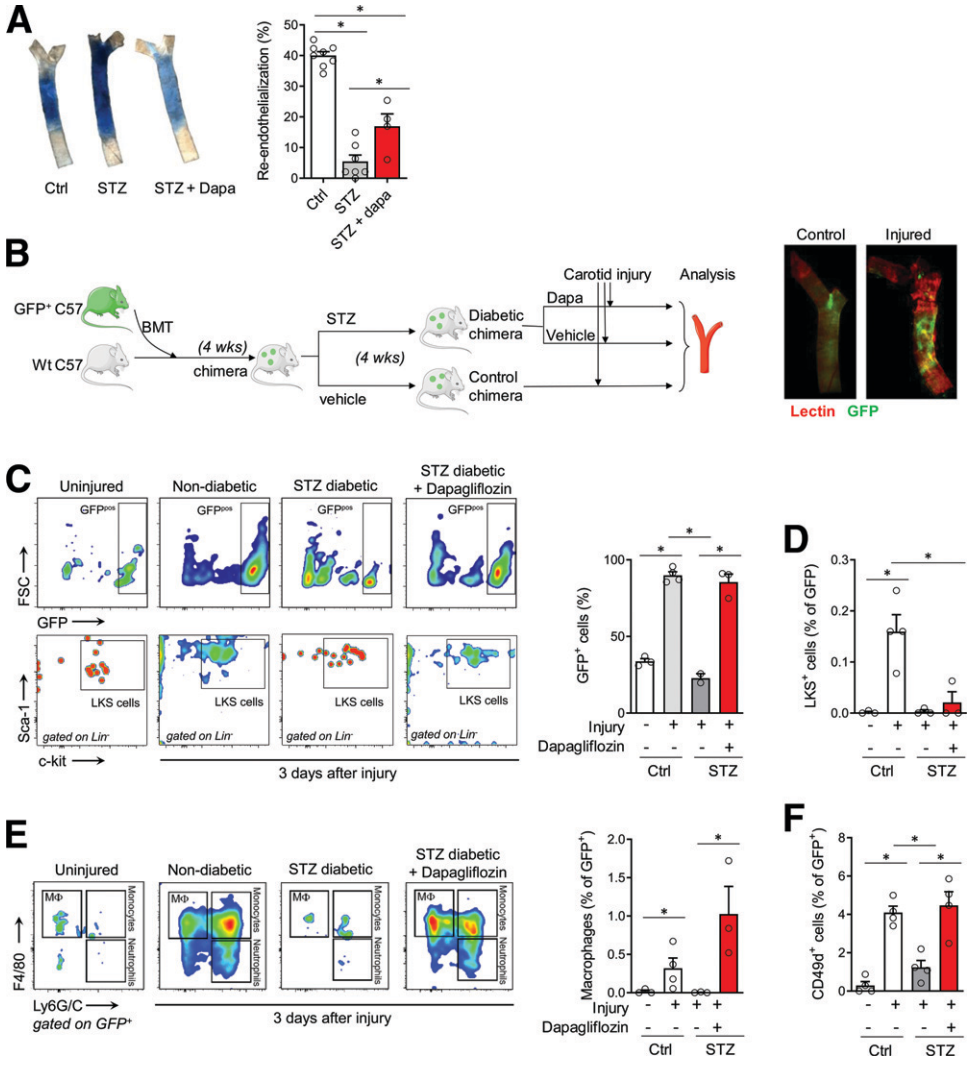

Figure 4—Endothelial repair and homing of BM-derived cells. *A*: Endothelial healing in nondiabetic control (Ctrl) mice and in STZ-induced diabetic mice with or without dapagliflozin (Dapa) treatment: the left panel shows Evans blue staining used to quantify the degree of residual endothelial denudation at day 3 after injury. Greater blue staining indicates lower re-endothelization, while less staining indicates greater repair. The right panel in *A* shows quantification of the degree of re-endothelization as percentage of the damaged area. *B*: Strategy to generate BM GFP chimeras, induction of diabetes by STZ, treatment with dapagliflozin or vehicle, and creation of endothelial damage. The microphotographs on the right show proof-of-concept demonstration of abundant GFP$^+$ cells physically recruited to the injured carotid arteries, compared with the uninjured contralateral carotid, showing autofluorescence or GFP signal at the bifurcation (possible sign of homing to site of shear stress-induced injury). *C*: Quantification of the amount of GFP$^+$ BM-derived cells within the carotid arteries of uninjured, nondiabetic, and STZ diabetic with or without dapagliflozin treatment: the left panel shows representative flow cytometry plots, while the right panel shows quantification of the percentage of GFP$^+$ cells over total tissue cellularity. *D*: Quantification of antigenically defined GFP$^+$ HSPCs (LKS cells) in the carotid arteries of the same group of mice. *E*: Mature GFP$^+$ cells homed from the BM to the carotid arteries were further characterized as monocytes, macrophages, or neutrophils based on the expression of F4/80 and Ly6C/G: the left panel shows representative plots, while quantification of macrophages is provided in the right panel. *F*: Neutrophils were further characterized for expression of the proangiogenic marker CD49d and percentage of CD49d$^+$ neutrophils over total GFP$^+$ cells are shown in the various groups. Histograms show mean values, SEs, and superimposed individual data points. One-way ANOVA was used (*$P <$ 0.05 for the indicated post hoc comparisons). BMT, BM transplant; FSC, forward scatter.

AMD3100, at a concentration (?0.5 μmol/L) expected to be achieved in plasma after the in vivo dose we used (30), inhibited a typical intracellular signal CXCR4 elicited by the ligand CXCL12 (i.e., AKT phosphorylation on serine-473) (Fig. 6*A* and *B*) As expected, AMD3100 impaired in vivo endothelial healing at day 3 after carotid injury in nondiabetic mice. However, AMD3100 did not modify the effects of dapagliflozin on the recovery of endothelial healing in STZ diabetic mice (Fig. 6*C* and *D*). Notably, using BM-GFP$^+$ chimeric mice, we found that AMD3100 impaired re-endothelization without affecting the homing of BM-derived cells in nondiabetic mice (Fig. 6*E*).

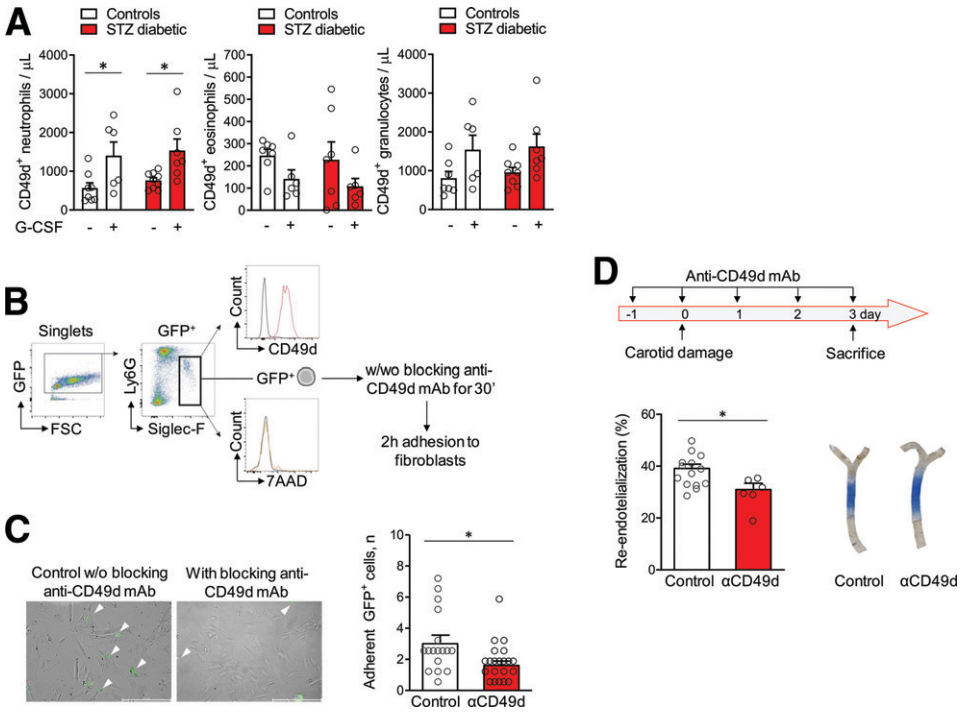

Figure 5—Adhesion of CD49d$^+$ neutrophils is required for endothelial healing. *A*: Mobilization of CD49d$^+$ neutrophils (left), eosinophils (middle), and total granulocytes (right) induced by G-CSF in nondiabetic control mice and in mice with STZ-induced diabetes. *B*: Identification and isolation of Ly6G^{low}Siglec-F$^+$ cells enriched for CD49d expression by flow cytometry from GFP-expressing mice and strategy for blocking CD49d with neutralizing mAb. *C*: Adhesion of Ly6G^{low}Siglec-F$^+$ cells enriched for CD49d$^+$ cells to fibroblasts with and without anti-CD49d–blocking mAb. Panel on the right shows quantification of adhering GFP$^+$ cells. *D*: The top panel illustrates the experiment performed to block adhesion of CD49d cells by in vivo injection of blocking mAb. The bottom panel in *D* shows quantification of re-endothelization 3 days after carotid damage with or without blocking antibody anti-CD49d (αCD49d), with representative microphotographs. Histograms show mean values, SEs, and superimposed individual data points (*$P < 0.05$ for the indicated post hoc comparisons). 7AAD, 7-aminoactinomycin D; FSC, forward light scatter; w/wo, with/without; w/o, without.

Systemic Mechanisms of Improved HSPC Traffic and Vascular Repair

In view of the very low gene expression of SGLT2 on extrarenal tissues without protein detection and on the limited effects of dapagliflozin on hematopoiesis in baseline conditions, we hypothesized that the effects exerted by dapagliflozin on BM-derived cell traffic may be mediated at a systemic level. EPO regulates the mobilization of hematopoietic cells with vascular repair capacity (31,32), and red cell mass has been implicated in cardiovascular protection by SGLT2i (9,10). Thus, we first examined if dapagliflozin increased EPO gene expression and release. There was a trend toward increased EPO gene expression in the kidney of STZ diabetic mice and of increased plasma EPO concentrations. However, dapagliflozin exerted no significant effect on EPO gene expression (Supplementary Fig. 6*A*). Plasma EPO concentrations were significantly increased by dapagliflozin in nondiabetic mice but not in STZ diabetic mice (Supplementary Fig. 6*B*).

Since any systemic effect of SGLT2i cannot be separated from the improvement in blood glucose, we tested if insulin therapy mimicked the effects of dapagliflozin. We treated STZ diabetic mice with low-dose basal insulin to achieve a degree of glucose control that was similar to that obtained with dapagliflozin. At the end of treatment, blood glucose was reduced by 25% in insulin-treated mice compared with vehicle-treated mice but was still markedly elevated (on average 437 vs. 579 mg/dL) (Fig. 7*A*). Insulin also induced a recovery of body weight (Fig. 5*B*). HSPC mobilization after G-CSF was partially rescued in insulin-treated diabetic mice to an extent similar to that obtained with dapagliflozin (4.5 ± 1.7-fold increase) (Fig. 7*C* and *D*). Interestingly, insulin treatment also improved re-endothelization after carotid injury (Fig. 7*E*). These results suggest that the effects observed with dapagliflozin may be mediated, at least in part, by an improved glucose control.

Finally, we examined if ketogenesis induced by dapagliflozin played any role on HSPC traffic. To this end, we administered mice with a ketone drink to achieve the same blood levels of ketone bodies observed during dapagliflozin. With both dapagliflozin and the ketone drink, BOHB concentrations were increased about threefold compared with those observed in untreated diabetic mice (Fig. 7*F*), yet at much lower levels (?0.3 mmol/L) than those typically occurring during human diabetic ketoacidosis. The ketone drink exerted no effect on glucose levels (Fig. 7*G*). In this condition, HSPC mobilization after stimulation

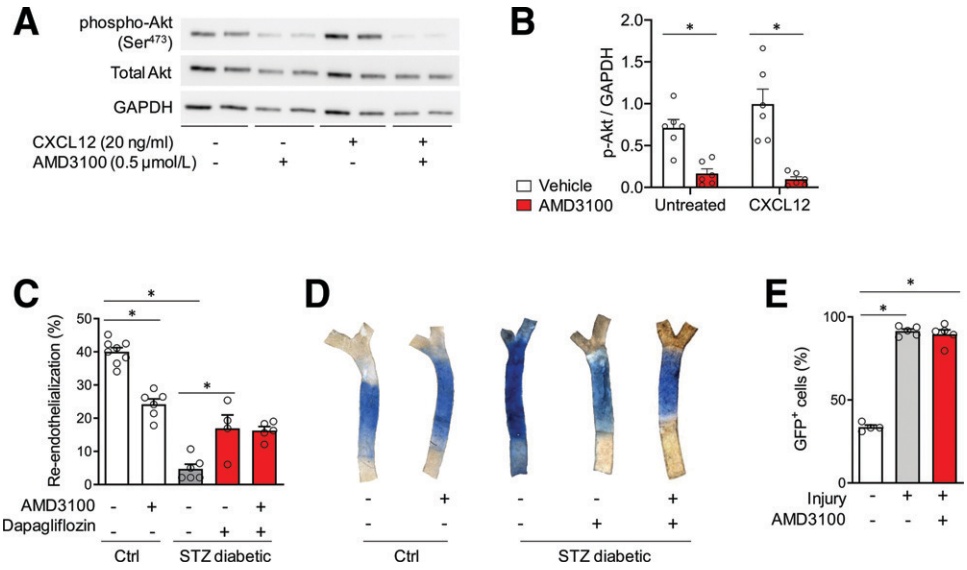

Figure 6—Effects of low-dose AMD3100 on endothelial healing. *A*: CXCR4 antagonism with AMD3100 0.5 μmol/L blocked phosphorylation of Akt on serine-473 in the presence or in the absence of CXCR4 agonist CXCL12 in HUVECs. *B*: Quantification of the phospho-Akt (p-Akt) over GAPDH in unstimulated or CXCL12-stimulated HUVECs with or without AMD3100. *C*: Effect of AMD3100 on endothelial repair, evaluated by Evans blue staining, in nondiabetic control (Ctrl) or STZ-induced diabetic mice with or without dapagliflozin treatment. *D*: Representative microphotographs of carotid arteries stained with Evans blue from the five groups. *E*: Percentage of GFP$^+$ cells over total cellularity in injured carotids or contralateral uninjured carotids with or without AMD3100 treatment in nondiabetic BM-GFP$^+$ chimeras. Histograms show mean values, SEs, and superimposed individual data points (*$P < 0.05$ for the indicated post hoc comparisons).

with G-CSF was rescued to 4.5 ± 0.4-fold in diabetic mice (Fig. 7*H* and *I*). Furthermore, artificial elevation of BOHB with the ketone drink led to an improvement in the extent of carotid endothelial healing in diabetic mice (Fig. 7*J*) that was similar to that observed with dapagliflozin.

DISCUSSION

The mechanisms by which SGLT2i improves cardiovascular outcomes remains largely unknown (4). Alterations in BM-derived cell kinetics, resulting in the pauperization of circulating HSPCs, contribute to micro- and macrovascular diabetic complications. In this study, we show that therapy with the SGLT2i dapagliflozin was able to reverse, at least in part, mobilization and homing of BM-derived cells to sites of vascular damage, thereby improving endothelial repair.

We used the T1D-like mouse model because it is associated with a complete defect in HSPC mobilization and a severe impairment in vascular healing, whereas the same could not be shown for a T2D-like model. Although initially developed for the treatment of T2D, dapagliflozin can also be used for T1D because its glucose-lowering action is independent from insulin secretion (33). Furthermore, there is solid demonstration that cardiorenal benefits of SGLT2i, which were initially shown in patients with T2D (3,34), also apply to individuals without diabetes (35,36). To minimize the confounding role of glucose control, we chose a lower dapagliflozin dose than that needed to normalize glucose levels in mice. Indeed, most extraglycemic effects of SGLT2i are independent from the degree of glucose control (35,37).

In STZ-induced diabetes, the complete unresponsiveness to G-CSF is ideal to test pharmacologic strategies to rescue HSPC mobilization and improve complications. The observation that SGLT2 is expressed in the BM, though at low levels, provides a rationale for evaluating the effects of dapagliflozin on BM cell traffic. In agreement with the notion that CD169$^+$ macrophages retain HSPCs in the BM niche (38), dapagliflozin prevented the increase in CD169$^+$ macrophages seen in diabetic mice and recovered the surge in HSPCs after G-CSF toward normal levels. CD169$^+$ macrophages display proinflammatory M1 features (25), which rely on glycolytic metabolism (39). We speculate that attenuation of diabetes-induced raise in CD169$^+$ macrophages by dapagliflozin resulted from blunting myelopoiesis though specific metabolic effects, including induction of ketogenesis, which may counter M1 polarization (40).

We then evaluated if improving the traffic of BM-derived cells would translate into vascular benefits. We used an endothelial injury model in which healing relies on two processes: *1*) activation of local endothelial cells; and *2*) recruitment of circulating BM-derived cells (28,41) that we tracked in BM-GFP$^+$ chimeric mice. Diabetes strongly reduced homing of BM-derived cells to the injured endothelium and delayed healing. Treatment of diabetic mice with dapagliflozin rescued homing of BM-derived cells and improved endothelial healing. Interestingly, among mature cells homed to

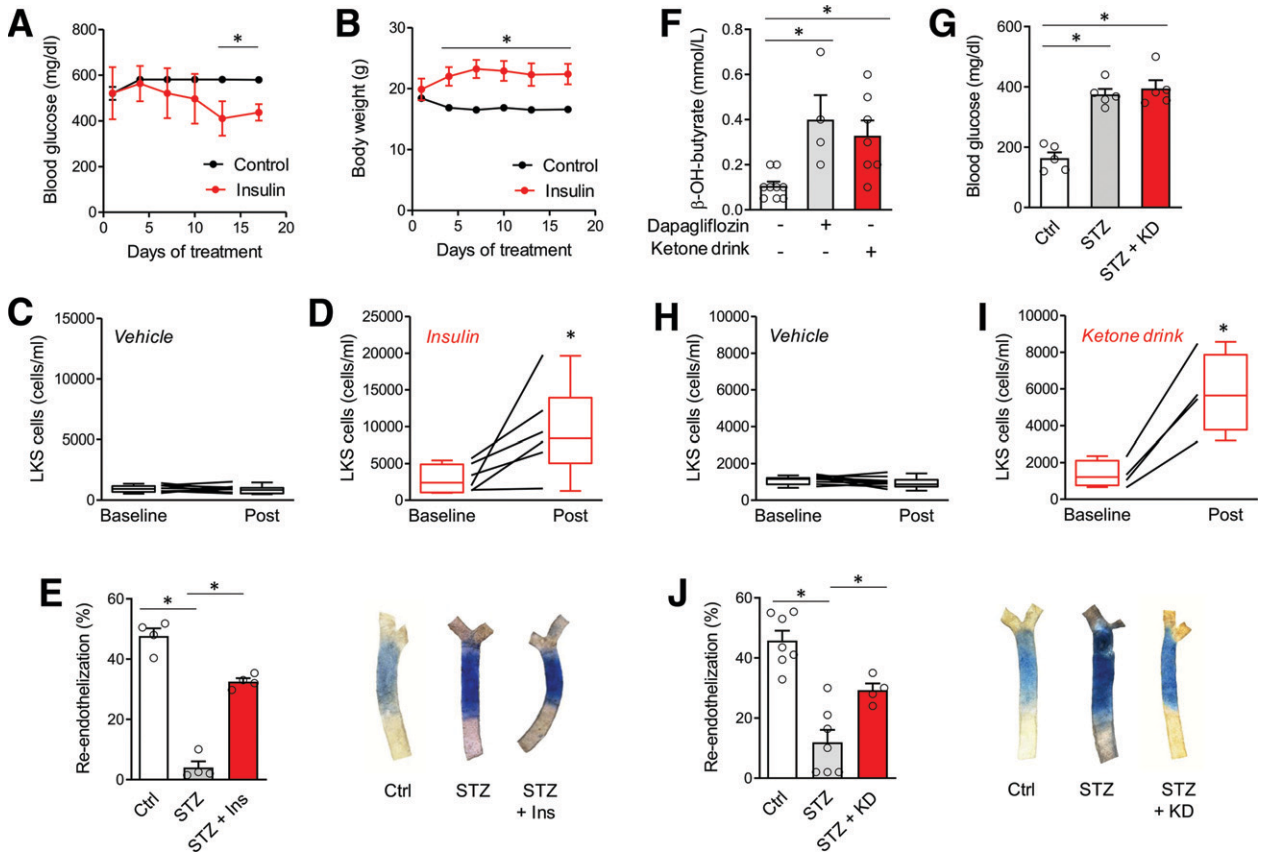

Figure 7—Effects of isoglycemic insulin treatment and ketone drink. *A*: A protocol was devised to achieve a degree of glucose control that was similar (isoglycemic) to that obtained with dapagliflozin in STZ-induced diabetic mice (*$P < 0.05$ upon point-by-point comparison between the two groups). *B*: Body weight change over time in STZ diabetic mice with or without insulin treatment (*$P < 0.05$ upon point-by-point comparison between the two groups). Mobilization of antigenically defined HSPCs (LKS cells) in STZ diabetic mice treated with vehicle (*C*) or insulin (*D*). *E*: Carotid re-endothelization after damage in nondiabetic control (Ctrl) mice and in STZ diabetic mice treated with vehicle or insulin (Ins). The right panel in *E* shows representative microphotographs of carotid arteries stained with Evans blue from the three groups. *F*: Concentrations of BOHB (β-OH-butyrate) in mice with STZ diabetes receiving vehicle, dapagliflozin, or a ketone drink (KD). *G*: Blood glucose concentrations in control mice (Ctrl) and in mice with STZ diabetes with or without treatment with a KD. *H* and *I*: Mobilization of HSPCs (LKS cells) in mice with STZ diabetes treated with vehicle or a KD. *J*: Carotid re-endothelization after damage in nondiabetic control (Ctrl) mice and in STZ diabetic mice treated with vehicle or a KD. The right panel in *J* shows representative microphotographs of carotids stained with Evans blue from the three groups. Plots in *C*, *D*, *H*, and *I* show median (line), interquartile range (box), and range (whiskers) with connecting lines representing individual mice (*$P < 0.05$ post vs. baseline upon paired test). Histograms show mean values, SEs, and superimposed individual data points (*$P < 0.05$ for the indicated comparisons).

the vasculature, dapagliflozin was particularly effective in increasing the amount of CD49d$^+$ granulocytes. We have recently shown that CD49d$^+$ granulocytes exert proangiogenic activities and are reduced in the blood of murine and human diabetes, possibly due to impaired generation from BM precursors (27). Of note, we already observed that dapagliflozin increased the levels of circulating CD49d$^+$ granulocytes in patients with diabetes (27), and we now show that it can improve their homing to sites of vascular damage. Remarkably, artificially inhibiting CD49d cell adhesion by blocking antibodies prevented normal endothelial healing. Therefore, the ability of dapagliflozin to rescue recruitment of CD49d$^+$ granulocytes can be mechanistically linked to the improved endothelial repair.

Although endothelial repair was significantly improved by dapagliflozin, it was still lower than in nondiabetic mice, suggesting that only part of the defect was countered. We thus wanted to understand the relative contribution of resident and circulating cells to the degree of endothelial repair promoted by dapagliflozin. We found that blocking CXCR4 with low-dose AMD3100 reduced endothelial healing in nondiabetic mice without affecting BM-derived cell mobilization and homing, thereby arguably acting on resident endothelial cells. Of note, AMD3100 did not abolish the beneficial effect of dapagliflozin on endothelial repair in diabetic mice. Thus, the partial improvement in re-endothelization by dapagliflozin can be explained by a recovery of BM-derived cell homing without an effect on resident endothelial cells, which, otherwise, would be prevented by concomitant treatment with AMD3100.

Although the SGLT2 gene was expressed in the BM, its levels were 10^{-4} times lower than in the kidney, and the protein could not be detected, implying that a strong

effect of dapagliflozin on the BM independently from the effect on the kidney seems unlikely. We thus explored whether systemic changes that are typically induced by SGLT2i through its action on the kidney could mimic the effects observed with dapagliflozin. After ruling out a substantial effect on EPO, we focused on glucose control to evaluate if the mild glycemic improvement induced by low-dose dapagliflozin was at least in part responsible for the improved BM-derived cell traffic and vascular repair. Using a protocol of insulin therapy that reproduced the same degree of glucose reduction obtained with dapagliflozin, we observed a similar improvement in HSPC mobilization and endothelial repair. These data suggest that the mild improvement in glucose control during dapagliflozin might have contributed to the observed effects on BM cell traffic and vascular repair. Yet, glucose levels were far from normal, and a direct effect of insulin on the BM and vascular repair cannot be ruled out (42). Furthermore, body weight effects were strikingly different between dapagliflozin and insulin therapy. In fact, STZ-induced diabetes in mice leads to weight loss, a feature of starvation that can be affected by SGLT2i (43) and insulin in opposite ways. Of note, the same results seen with dapagliflozin and insulin were mimicked by treating mice with a ketone drink to achieve similar levels of ketone body elevation as observed during dapagliflozin, without lowering glucose levels. Lactate has been recently shown to regulate BM-cell traffic (44), so that similar effects may be carried out by BOHB. The molecular and metabolic pathways involved in these findings are particularly intriguing and deserve further investigation. Overall, our data are consistent with the view that multiple metabolic effects, carried out at a systemic level, are likely involved.

In summary, we uncover a new mechanism by which dapagliflozin could exert beneficial effects on the macro- and microvasculature. By rescuing mobilization of immature cells from BM to the bloodstream and by improving homing of mature cells to sites of vascular damage, dapagliflozin promoted endothelial healing. Such recovery of endogenous repair is likely to be carried out through multiple mechanisms, including the improvement of glucose control and the induction of ketogenesis.

Funding. This study was supported by grants from: University of Padova (DOR), Ministry of University and Education (PRIN projects 2015ZTT5KB and 201793XZ5A) and AstraZeneca (NCR-17-12732).

The external sponsor had no role in study design, conduction, data analysis, interpretation, and decision to publish.

Duality of Interest. A.A. and G.P.F. received honoraria or lecture fees from AstraZeneca, Boehringer Ingelheim, Mundipharma, and MSD, the manufacturers of SGLT2i. No other potential conflicts of interest relevant to this article were reported.

Author Contributions. M.A. performed experiments, researched and analyzed data, and wrote the manuscript. S.T. performed experiments, researched and analyzed data, and revised the manuscript. F.I.A. performed experiments, researched and analyzed data, and revised the manuscript. M.D'.A. performed experiments, researched and analyzed data, and revised the manuscript. L.M. performed experiments, researched and analyzed data, and revised the manuscript. G.Z. performed experiments, researched and analyzed data, and revised the manuscript. A.R. designed experiments, contributed to discussion, and revised the manuscript. R.C. performed experiments, researched and analyzed data, and revised the manuscript. A.A. provided supervision and funding, contributed to discussion, and revised the manuscript. G.P.F. researched and analyzed data, provided supervision and funding, and wrote the manuscript. M.A. and G.P.F. are the guarantors of this work and, as such, had full access to all of the data in the study and take responsibility for the integrity of the data and the accuracy of the data analysis.

References

1. Rao Kondapally Seshasai S, Kaptoge S, Thompson A, et al.; Emerging Risk Factors Collaboration. Diabetes mellitus, fasting glucose, and risk of cause-specific death. N Engl J Med 2011;364:829–841

2. Boussageon R, Bejan-Angoulvant T, Saadatian-Elahi M, et al. Effect of intensive glucose lowering treatment on all cause mortality, cardiovascular death, and microvascular events in type 2 diabetes: meta-analysis of randomised controlled trials. BMJ 2011;343:d4169

3. Zelniker TA, Wiviott SD, Raz I, et al. SGLT2 inhibitors for primary and secondary prevention of cardiovascular and renal outcomes in type 2 diabetes: a systematic review and meta-analysis of cardiovascular outcome trials. Lancet 2019;393:31–39

4. Lopaschuk GD, Verma S. Mechanisms of cardiovascular benefits of sodium glucose co-transporter 2 (SGLT2) inhibitors: a state-of-the-art review. JACC Basic Transl Sci 2020;5:632–644

5. Kuo S, Ye W, Duong J, Herman WH. Are the favorable cardiovascular outcomes of empagliflozin treatment explained by its effects on multiple cardiometabolic risk factors? A simulation of the results of the EMPA-REG OUTCOME trial. Diabetes Res Clin Pract 2018;141:181–189

6. Verma A, Patel AB, Waikar SS. SGLT2 inhibitor: not a traditional diuretic for heart failure. Cell Metab 2020;32:13–14

7. Zinman B, Wanner C, Lachin JM, et al.; EMPA-REG OUTCOME Investigators. Empagliflozin, cardiovascular outcomes, and mortality in type 2 diabetes. N Engl J Med 2015;373:2117–2128

8. Mazer CD, Hare GMT, Connelly PW, et al. Effect of empagliflozin on erythropoietin levels, iron stores, and red blood cell morphology in patients with type 2 diabetes mellitus and coronary artery disease. Circulation 2020;141:704–707

9. Inzucchi SE, Zinman B, Fitchett D, et al. How does empagliflozin reduce cardiovascular mortality? Insights from a mediation analysis of the EMPA-REG OUTCOME Trial. Diabetes Care 2018;41:356–363

10. Li J, Woodward M, Perkovic V, et al. Mediators of the effects of canagliflozin on heart failure in patients with type 2 diabetes. JACC Heart Fail 2020;8:57–66

11. Uthman L, Baartscheer A, Bleijlevens B, et al. Class effects of SGLT2 inhibitors in mouse cardiomyocytes and hearts: inhibition of Na^+/H^+ exchanger, lowering of cytosolic Na^+ and vasodilation. Diabetologia 2018;61:722–726

12. Ferrannini E, Mark M, Mayoux E. CV protection in the EMPA-REG OUTCOME Trial: a "thrifty substrate" hypothesis. Diabetes Care 2016;39:1108–1114

13. Santos-Gallego CG, Requena-Ibanez JA, San Antonio R, et al. Empagliflozin ameliorates adverse left ventricular remodeling in nondiabetic heart failure by enhancing myocardial energetics. J Am Coll Cardiol 2019;73:1931–1944

14. Fadini GP, Ciciliot S, Albiero M. Concise review: perspectives and clinical implications of bone marrow and circulating stem cell defects in diabetes. Stem Cells 2017;35:106–116

15. Fadini GP, Mehta A, Dhindsa DS, et al. Circulating stem cells and cardiovascular outcomes: from basic science to the clinic. Eur Heart J 2020;41:4271–4282

16. Fadini GP, DiPersio JF. Diabetes mellitus as a poor mobilizer condition.-Blood Rev 2018;32:184–191

17. DiPersio JF. Diabetic stem-cell "mobilopathy". N Engl J Med 2011;365:2536–2538
18. Albiero M, Ciciliot S, Tedesco S, et al. Diabetes-associated myelopoiesis drives stem cell mobilopathy through an OSM-p66Shc signaling pathway. Diabetes 2019;68:1303–1314
19. Albiero M, Fadini GP. Pharmacologic targeting of the diabetic stem cell mobilopathy. Pharmacol Res 2018;135:18–24
20. Hess DA, Terenzi DC, Trac JZ, et al. SGLT2 inhibition with empagliflozin increases circulating provascular progenitor cells in people with type 2 diabetes mellitus. Cell Metab 2019;30:609–613
21. Fadini GP. SGLT-2 inhibitors and circulating progenitor cells in diabetes. Cell Metab 2020;31:883
22. Bonora BM, Cappellari R, Albiero M, Avogaro A, Fadini GP. Effects of SGLT2 inhibitors on circulating stem and progenitor cells in patients with type 2 diabetes. J Clin Endocrinol Metab 2018;103:3773–3782
23. Diabetic Complications Consortium. High-Dose STZ Induction Protocol (Mouse). Accessed April 26, 2021. Available from https://www.diacomp.org/shared/document.aspx?id=74&docType=Protocol
24. Nagareddy PR, Murphy AJ, Stirzaker RA, et al. Hyperglycemia promotes myelopoiesis and impairs the resolution of atherosclerosis. Cell Metab 2013;17:695–708
25. Albiero M, Poncina N, Ciciliot S, et al. Bone marrow macrophages contribute to diabetic stem cell mobilopathy by producing oncostatin M. Diabetes 2015;64:2957–2968
26. Vasam G, Joshi S, Jarajapu YP. Impaired mobilization of vascular reparative bone marrow cells in streptozotocin-induced diabetes but not in leptin receptor-deficient *db/db* mice. Sci Rep 2016;6:26131
27. Cappellari R, D'Anna M, Menegazzo L, et al. Diabetes mellitus impairs circulating proangiogenic granulocytes. Diabetologia 2020;63:1872–1884
28. Brenner C, Kränkel N, Kühlenthal S, et al. Short-term inhibition of DPP-4 enhances endothelial regeneration after acute arterial injury via enhanced recruitment of circulating progenitor cells. Int J Cardiol 2014;177:266–275
29. Noels H, Zhou B, Tilstam PV, et al. Deficiency of endothelial CXCR4 reduces reendothelialization and enhances neointimal hyperplasia after vascular injury in atherosclerosis-prone mice. Arterioscler Thromb Vasc Biol 2014;34:1209–1220
30. Datema R, Rabin L, Hincenbergs M, et al. Antiviral efficacy in vivo of the anti-human immunodeficiency virus bicyclam SDZ SID 791 (JM 3100), an inhibitor of infectious cell entry. Antimicrob Agents Chemother 1996;40:750–754
31. Brunner S, Winogradow J, Huber BC, et al. Erythropoietin administration after myocardial infarction in mice attenuates ischemic cardiomyopathy associated with enhanced homing of bone marrow-derived progenitor cells via the CXCR-4/SDF-1 axis. FASEB J 2009;23:351–361
32. Urao N, Okigaki M, Yamada H, et al. Erythropoietin-mobilized endothelial progenitors enhance reendothelialization via Akt-endothelial nitric oxide synthase activation and prevent neointimal hyperplasia. Circ Res 2006;98:1405–1413
33. Dandona P, Mathieu C, Phillip M, et al.; DEPICT-1 Investigators. Efficacy and safety of dapagliflozin in patients with inadequately controlled type 1 diabetes (DEPICT-1): 24 week results from a multicentre, double-blind, phase 3, randomised controlled trial. Lancet Diabetes Endocrinol 2017;5:864–876
34. Neuen BL, Young T, Heerspink HJL, et al. SGLT2 inhibitors for the prevention of kidney failure in patients with type 2 diabetes: a systematic review and meta-analysis. Lancet Diabetes Endocrinol 2019;7:845–854
35. McMurray JJV, Solomon SD, Inzucchi SE, et al.; DAPA-HF Trial Committees and Investigators. Dapagliflozin in patients with heart failure and reduced ejection fraction. N Engl J Med 2019;381:1995–2008
36. Heerspink HJL, Stefánsson BV, Correa-Rotter R, et al.; DAPA-CKD Trial Committees and Investigators. Dapagliflozin in patients with chronic kidney disease. N Engl J Med 2020;383:1436–1446
37. Wiviott SD, Raz I, Bonaca MP, et al.; DECLARE–TIMI 58 Investigators. Dapagliflozin and cardiovascular outcomes in type 2 diabetes. N Engl J Med 2019;380:347–357
38. Chow A, Lucas D, Hidalgo A, et al. Bone marrow CD169+ macrophages promote the retention of hematopoietic stem and progenitor cells in the mesenchymal stem cell niche. J Exp Med 2011;208:261–271
39. Viola A, Munari F, Sánchez-Rodríguez R, Scolaro T, Castegna A. The metabolic signature of macrophage responses. Front Immunol 2019;10:1462
40. Miyachi Y, Tsuchiya K, Shiba K, et al. A reduced M1-like/M2-like ratio of macrophages in healthy adipose tissue expansion during SGLT2 inhibition. Sci Rep 2018;8:16113
41. Kuschnerus K, Straessler ET, Müller MF, Lüscher TF, Landmesser U, Kränkel N. Increased expression of miR-483-3p impairs the vascular response to injury in type 2 diabetes. Diabetes 2019;68:349–360
42. Oikonomou D, Kopf S, von Bauer R, et al. Influence of insulin and glargine on outgrowth and number of circulating endothelial progenitor cells in type 2 diabetes patients: a partially double-blind, randomized, three-arm unicenter study. Cardiovasc Diabetol 2014;13:137
43. Packer M. Role of ketogenic starvation sensors in mediating the renal protective effects of SGLT2 inhibitors in type 2 diabetes. J Diabetes Complications 2020;34:107647
44. Khatib-Massalha E, Bhattacharya S, Massalha H, et al. Lactate released by inflammatory bone marrow neutrophils induces their mobilization via endothelial GPR81 signaling. Nat Commun 2020;11:3547